Rev.Adv.Mater.Sci. 6 (2004) 140-149

NANOSTRUCTURED COPPER/HYDROGENATED AMORPHOUS CARBON COMPOSITE FILMS PREPARED BY MICROWAVE PLASMA-ASSISTED DEPOSITION PROCESS FROM ACETYLENE-ARGON GAS MIXTURES

Y. Pauleau[1], F. Thiéry[1], P.B. Barna[2], F. Misjak[2], A. Kovacs[2], S.N. Dub[3], V.V. Uglov[4] and A.K. Kuleshov[4]

[1]National Polytechnic Institute of Grenoble, CNRS-LEMD, B.P. 166, 38042 Grenoble Cedex 9, France
[2]Research Institute for Technical Physics and Materials Science, Konkoly Thege ùt 29/33, 1121 Budapest, Hungary
[3]Institute for Superhard Materials, 2 Avtozavodskaya Str., 04074 Kiev, Ukraine
[4]Belarussian State University, Pr. F. Scoriny 4, 220080 Minsk, Belarus

Received: February 05, 2004

Abstract. Copper/carbon composite films have been deposited on Si substrates from argon-acetylene mixtures using a hybrid technique combining sputter-deposition and plasma-assisted chemical vapor deposition. The carbon content in these films determined by Rutherford backscattering spectroscopy was varied in the range 5-99 at.%. The crystallographic structure was determined by X-ray diffraction techniques. The microstructure of films was examined by transmission electron microscopy. The magnitude of compressive residual stresses increased up to 0.5 GPa with increasing carbon content in the films. The hardness and elastic recovery of films determined by nanoindentation measurements were studied as functions of the composition of the gas phase. Low friction coefficient values were obtained from films containing more than 50 at.% of carbon in room air with a relative humidity of 50%. The wear resistance of films containing 23 to 29 at.% of carbon was higher by a factor of 2 than that of pure Cu films.

1. INTRODUCTION

Diamond-like carbon (DLC) films can combine the properties of solid lubricating graphite structure and hard diamond crystal structure, i.e., extreme hardness approaching that of diamond, chemical inertness, high thermal conductivity and optical transparency without the crystalline structure of diamond. Hydrogenated and hydrogen-free DLC films prepared by various deposition techniques such as plasma-enhanced chemical vapor deposition (PECVD) and sputtering possess excellent lubricating properties under specific sliding conditions [1,2]. Depending on the tribological test conditions, the friction coefficient can be less than 0.10 or even as low as 0.01 [3,4]. The formation of graphite-like transfer films in the sliding contact leads to a large decrease in wear rate of materials [5]. However, DLC films may exhibit severe limitations and drawbacks. A poor adhesion of DLC films to various substrates, in particular steel substrates result from the excessive magnitude of compressive residual stresses (several GPa) developed in hard DLC films. In addition, the thermal stability of DLC films is not sufficiently high for a given application (maximum temperature of 250 °C in operation) and the lubricating properties depend considerably on the environment [6-8].

Recently, hydrogen-free DLC films produced by pulsed laser deposition exhibited a superhardness in the range 60-70 GPa and the friction coefficient values were between 0.06 and 0.10 for a wide range of test environment [9,10]. The wear rate of these films was found to be several orders of magnitude lower than that of ceramic coatings [9,11]. However,

Corresponding author: Y. Pauleau, e-mail: yves.pauleau@grenoble.enrs.fr

fracture and delamination of films deposited on steel substrates were observed as the Hertzian contact pressure was above 1 GPa. The analyses of failures demonstrated that these superhard DLC films lacked toughness and resistance to cross-sectional crack propagation [12]. A possible method to improve film toughness would be through compositional modifications, e.g., incorporation of nanosized metal clusters in the DLC matrix to produce composite films or hydrogenation of amorphous carbon films.

The major pioneering works on carbide forming metal/hydrogenated amorphous carbon (a-C:H) composite films have been performed at the beginning of eighties by Dimigen *et al*. [2,13,14]. Small friction coefficients against steel or cemented carbide (WC/Co 6 wt.%) were obtained from Me/a-C:H composite films (with Me = Ta, W or Fe) deposited by reactive sputtering as the metal content in the films was less than 30 at.%. Recently, the tribological properties of titanium/carbon composite films were thoroughly investigated [15-17]. The technique named magnetron assisted pulsed laser deposition was used to prepare films of crystalline TiC, TiCN and hydrogen-free amorphous carbon (a-C) exhibiting characteristics of DLC films [18]. Pure TiC and a-C films exhibited high hardness values of 27 to 60 GPa, respectively [19]. The hardness of TiC/a-C composite films containing 30 at.% of Ti determined by nanoindentation under a load of 1 mN was about 32 GPa. This hardness is higher than that of nanocrystalline stoichiometric TiC films but not so high as the hardness of 60 GPa for sp^3-bonded a-C films. However, the ductility of these TiC/a-C composite films deduced from nanoindentation tests was equal to 40%, i.e., four times higher than that of superhard but brittle a-C films. To explain the observed combination of high hardness and elevated ductility, various arguments were proposed and developed by Voevodin *et al*. [19,20].

Metal/carbon composite films combining high hardness, elevated ductility and toughness are recognized to be of interest as wear-resistant and low friction films for tribological applications [21]. Toughness can be achieved by strain release via nanosized metal-based crystallites sliding in the amorphous carbon matrix. In metal/carbon composite films containing metal such as Cu or Ag inert with respect to carbon, crystallite-carbon interfaces are expected to be very abrupt with very weak interaction forces. Under these conditions, the deformation at grain boundaries or metal-carbon interfaces leading to multiple shifts of nanocrystallites with respect to one another should be facilitated as a stress is applied. These Cu/C or Ag/C composite films may have high ductility and toughness. Furthermore, the tribological behavior and friction properties of these metal/carbon composite films can be very distinct from those of carbide forming metal/carbon composite films.

Phase segregation phenomena are required for the formation of nanosized metal clusters in the carbon matrix during film growth. The appropriate deposition technique should assure sufficiently energy for the thermodynamically driven segregation of the phase to occur [22]. Activated chemical or physical vapor deposition (CVD or PVD) techniques, in particular plasma-assisted CVD and PVD appear to be suitable for preparation of metal/carbon composite films. Copper/amorphous carbon or polymer composite films of a variety of compositions have been deposited by various techniques including co-evaporation [23,24], ion implantation [25,26], ion beam deposition [27], pulsed laser ablation [28], co-sputtering [29-33], reactive sputtering [34-37] and hybrid technique combining microwave PECVD of carbon from argon-methane or acetylene mixtures and sputtering of a Cu target [38,39].

The purpose of the present paper is to report on the results of experiments designed to prepare Cu/a-C:H composite films by microwave plasma-assisted deposition techniques and to investigate the composition, microstructure, mechanical properties and tribological behavior of composite films produced from argon-acetylene mixtures of various compositions.

2. EXPERIMENTAL

Copper/carbon composite films have been deposited on (100)-oriented single crystal silicon substrates mounted on a water-cooled substrate holder. The deposition of films was carried out using a distributed electron cyclotron resonance (DECR) microwave plasma reactor [40], i.e., a hybrid technique combining DECR microwave plasma-assisted chemical vapor deposition and sputtering of a metal target from argon-hydrocarbon mixtures. The deposition set-up and experimental procedure were described recently [41,42]. Briefly, the microwave field was applied through four cylindrical antennae of 8 mm in diameter placed at the periphery of the cylindrical plasma chamber. The total microwave power was maintained at 400 W. The metal target of 100 mm in diameter was biased to – 300 V and – 600 V for deposition of Cu/carbon and Ni/carbon films, respectively. The target-substrate distance was equal to 13 cm. The total pressure in the deposition chamber was fixed at 0.13 Pa while the methane concen-

tration in the gas phase was varied from 0 to 100%. The flow rates of argon and acetylene were varied in the range 0-10 cm^3/min. The water-cooled substrate holder was maintained at the floating potential. The duration of the deposition step was fixed at 30 min. The thickness of films was measured by surface profilometry.

The composition of films was determined by Rutherford backscattering spectroscopy (RBS) measurements. For determination of the copper content, the RBS measurements were performed using 2 MeV $^4He^+$ beam at normal incidence and the detection angle was equal to 160°. The carbon content was obtained from backscattering measurements using helium particles of 3.4 MeV. At this energy, the backscattering cross-section on carbon atoms is higher by a factor of 5 than the Rutherford value. As a result, the carbon peak in these NRBS (non-Rutherford backscattering) spectra emerged significantly above the base line corresponding to backscattering events on substrate atoms and the carbon content can be determined without any ambiguity. The hydrogen content was obtained from elastic recoil detection analyses (ERDA) using a 2.9 MeV $^4He^+$ beam and a glancing angle forward scattering geometry. The accuracy on the atom concentrations determined by RBS, NRBS and ERDA was in the range 1-5 at.%.

The crystallographic structure of films was determined by X-ray diffraction (XRD) techniques using an Inel diffractometer in θ-2θ position, with a collecting angle varying from 5° to 150°. The copper *K*a radiation (with wavelength of 1.5406 Å) was used to analyze the samples. The position and integral width of XRD peaks were determined to identify the crystalline phase and to calculate the size of smallest crystallites from the Scherrer equation, respectively [43].

The microstructure of films was examined by cross-sectional transmission electron microscopy (XTEM). The cross-sectional samples were prepared by mechanical grinding and a low angle, low energy ion-beam thinning technique [44]. The weak interface between the layers made XTEM sample preparation especially difficult because the layers were easily pulled apart.

The radius of curvature of Si substrates was measured prior and after deposition of films by surface profilometry. The magnitude of residual stresses in the films was calculated from the Stoney equation [45]. The mechanical properties of films were measured by nanoindentation using a Nano Indenter II (MTS Systems Corp.) equipped with a Berkovitch indenter. The load was varied in the range 0.25-50 mN. The hardness and elastic modulus were found at the minimal load using the Oliver and Pharr model [46].

The friction coefficient and wear resistance of films were investigated by pin-on-plane tribological tests with a reciprocating mode conducted in room air with a relative humidity of (50 ± 5) %. The pin was made of BK-8 hard alloy (87.5 HRC). The dry sliding speed and the normal load were equal to 4 mm/s and 1 N, respectively. The surface of wear tracks after various sliding distances was examined by optical microscopy.

3. RESULTS AND DISCUSSION

Pure copper films have been sputter-deposited from pure argon with a deposition rate of 26 nm/min under the experimental conditions investigated [47]. Copper/carbon composite films have been deposited on Si substrates covered with a native oxide layer by the microwave plasma-assisted hybrid deposition technique. The deposition rate of these composite films adherent to Si substrates was found to vary in the range (26-14) nm/min as the C_2H_2 concentration in the gas phase increased up to 100%. The thickness of films prepared under the deposition conditions investigated was varied from 420 and 780 nm.

3.1 Composition and structure of copper/carbon films

The composition of films expressed by the atom number ratios Cu/(Cu + C) and C/(Cu + C) was dependent on the C_2H_2 concentration in the gas phase (Fig. 1). As the C_2H_2 concentration was varied from 10 to 90%, the carbon content increased progressively and continuously from 5 to 99 at.% while the Cu content decreased symmetrically. With C_2H_2 concentrations in the gas phase higher than 90%, the Cu content in the films was less than 1 at.%. Under these conditions, the sputtering yield of the Cu target was considerably reduced. Carbon bearing species from the plasma condensed both on the substrate and target surfaces. At the very beginning of the deposition process, the Cu target surface was carbon free and Cu atoms were ejected from the target. After a very short period of time, the target surface was covered with carbon species and the amount of Cu atoms sputtered from the target was negligible. As a result, the Cu incorporation in the films occurred essentially during this short period of time and the Cu content was not uniformly distributed through the films. The Cu and C con-

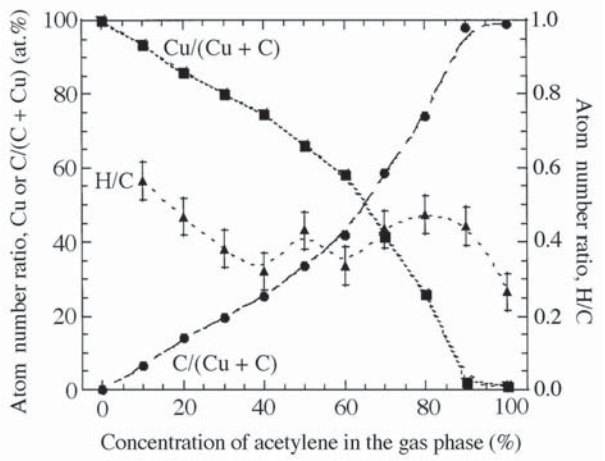

Fig. 1. Composition of Cu/a-C:H composite films versus C_2H_2 concentration in the gas phase.

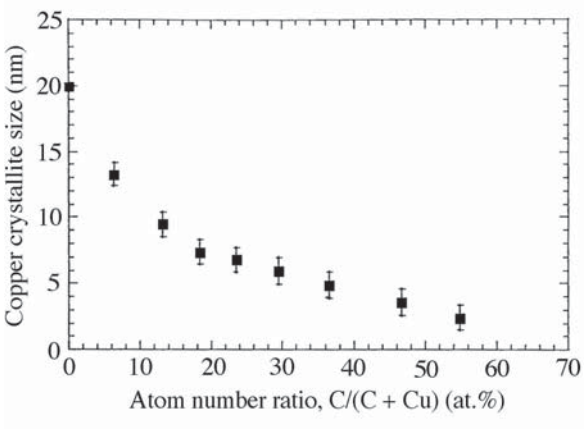

Fig. 2. Size of smallest copper crystallites embedded in the carbon matrix versus carbon content of films.

tents were equal in copper/carbon composite films deposited from a gas mixture containing 65% of C_2H_2.

The values of the atom number ratio H/C were relatively scattered between 0.25 and 0.55 depending on the gas phase composition (Fig. 1). The average value of this ratio was approximately equal to 0.40-0.45. In addition, this ratio H/C was significantly reduced in composite films containing less than 1 at.% of copper.

The major diffraction peaks in the X-ray diffraction patterns of Cu/a-C:H films were ascribable to the face-centered cubic (f.c.c.) copper phase [48]. The positions of the diffraction peaks (or diffraction angle values) were independent of the C_2H_2 concentration in the gas phase. As a result, the crystal lattice parameter of the copper phase was constant and independent of the composition of films consisting of polycrystalline copper and a-C:H phases. However, the intensities and widths of diffraction peaks were found to be dependent on the composition of films. The copper crystallite size was calculated from the integral width of the (111) diffraction peak using Scherrer equation (Fig. 2). For pure copper films, the crystallite size was about 20 nm. The copper crystallite size in Cu/a-C:H films decreased progressively and continuously from 20 to 2 nm as the carbon content increased up to 55 at.%. This value corresponds to the size of smallest copper crystallites incorporated in the films.

A typical XTEM image of Cu/a-C:H composite films is displayed in Fig. 3. The C content or the atom number ratio C/(Cu + C) in this film prepared from a gas mixture containing 20% of C_2H_2 was equal to approximately 15 at.%. The XTEM images revealed various structural details. The samples exhibited a continuous polycrystalline copper layer at the film-substrate interface and this copper layer was covered with the composite film. For the 600-nm-thick Cu/a-C:H film displayed in Fig. 3, the thickness of the copper film at the substrate surface was approximately 25 nm. This copper layer was grown during the first stage of the deposition process when the Cu target was not totally covered with a layer of carbon species. The C content in this layer was very low or negligible. As a result, segregation phenomena of Cu atoms and carbon species were probably very active during the growth of this copper film on the substrate surface. The upper part of the film exhibits a fine-grained structure with a uniform distribution of copper crystallites wrapped in an amorphous carbon tissue. According to the XRD data, the size of smallest copper crystallites incorporated in the upper part of film was approximately 7 nm.

3.2 Mechanical characteristics of copper/carbon films

The magnitude of tensile residual stresses developed in pure Cu films was less than 0.3 GPa [47]. The carbon incorporation in Cu films led to a reduction of the magnitude of residual stresses. For Cu/a-C:H films containing approximately 5 at.% of carbon, the residual stresses were negligible (Fig. 4). Residual stresses were found to be compressive in Cu/a-C:H films with a C content in the range 10-95 at.%; In addition, the magnitude of compressive re-

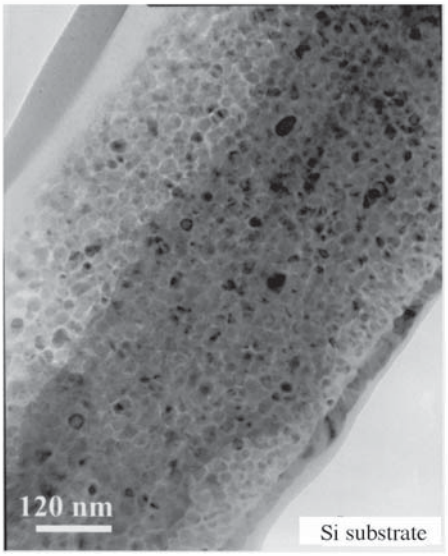

Fig. 3. Typical transmission electron micrograph on the cross-section of a Cu/a-C:H film deposited from a gas mixture containing 20% of acetylene.

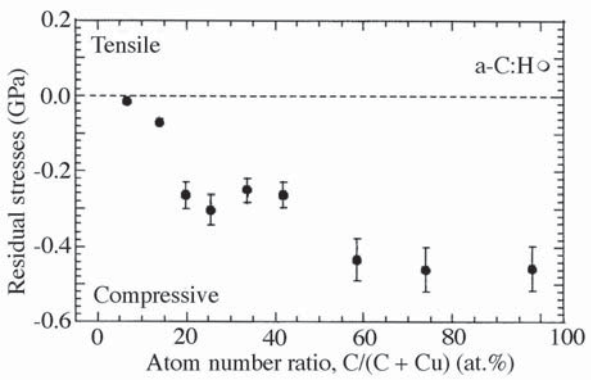

Fig. 4. Residual stresses developed in: (o) a-C:H films prepared by plasma-assisted chemical vapor deposition from pure C_2H_2 and (•) Cu/a-C:H films as a function of the carbon content in the films.

sidual stresses increased up to 0.5 GPa with increasing carbon content. The residual stresses developed in hydrogenated amorphous carbon (a-C:H) films produced by microwave plasma-enhanced chemical vapor deposition from pure acetylene were found to be tensile (Fig. 4). During deposition of these films, the target was not biased. As a result, no energetic species were ejected from the target surface and condensed on the surface of growing films. The substrates were at the floating potential and the difference between the plasma potential and the floating potential was equal to approximately 10 V whatever the gas phase composition. The relatively low kinetic energy (10 eV) of species condensed on substrates at the floating potential may be responsible for the growth of a-C:H films with tensile residual stresses [45]. The progressive development of compressive residual stresses in Cu/a-C:H films can be related to the kinetic energy of carbon species ejected from the target surface. The fraction of these energetic carbon species condensed on the surface of growing films increased with increasing C_2H_2 concentration in the gas phase.

Two groups of Cu/a-C:H films can be distinguished depending on the hardness values (Fig. 5). The first group of composite films was produced from gas mixtures containing 10 to 60% of C_2H_2. These films containing 10 to 40 at.% of carbon exhibited a similar hardness in the range 2-2.5 GPa. These hardness values are very similar to the hardness of pure Cu films produced by sputtering [42]. The load-displacement curves of these samples were similar at high peak loads and displayed a wide hysteresis loop during reloading (Fig. 6a). The width of the loop decreased with decreasing the loading rate. The wide hysteresis loop and its dependence on the loading rate, which are characteristic features of polymer-like materials, are caused by the viscoelastic mechanical behavior of these materials [49,50]. These Cu/a-C:H films belong to the so-called plasma polymer materials with the hardness of approximately 1 GPa deposited at room temperature un-

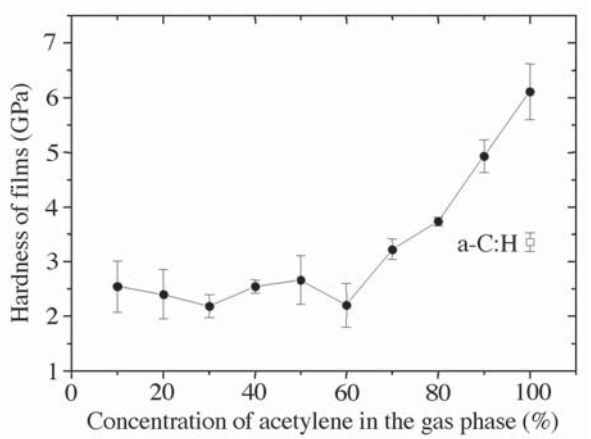

Fig. 5. Hardness of : (•) Cu/a-C:H films and (□) a-C:H films prepared by plasma-enhanced chemical vapor deposition from pure C_2H_2 as a function of the C_2H_2 concentration in the gas phase.

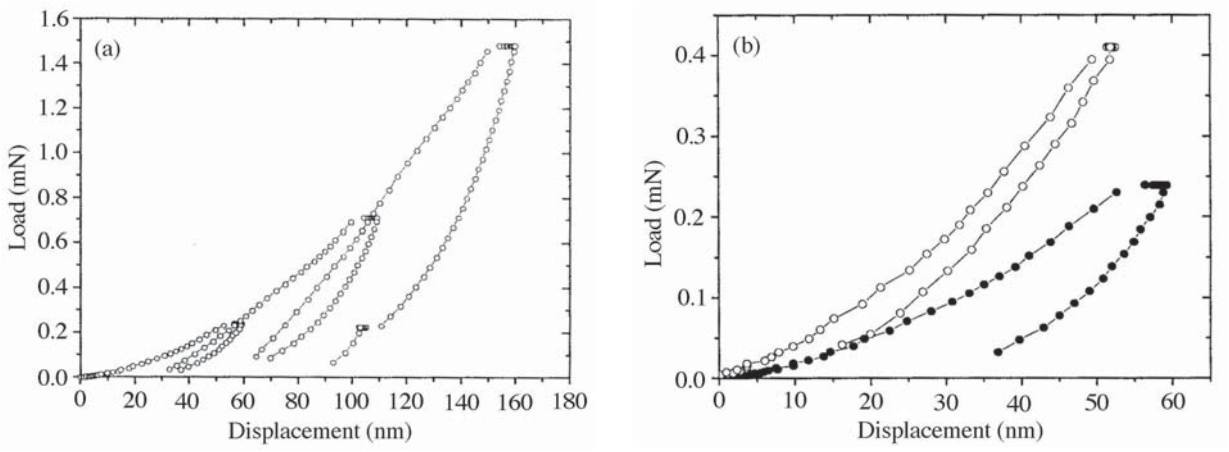

Fig. 6. a) Load-displacement curves of Cu/a-C:H films deposited from a gas mixture containing 60% of C_2H_2. The large hysteresis loops are characteristic of a soft polymer-like a-C:H matrix. b) First loading cycle for Cu/a-C:H films produced from a gas mixture containing : (•) 60% of C_2H_2 and (o) 100% of C_2H_2. The small hysteresis loop is characteristic of an ion-hardened a-C:H matrix.

der low energy bombardment [51]. The copper crystallites in these films resulted in increased hardness values up to 2.5 GPa.

The second group of samples consisted of Cu/a-C:H films deposited from gas mixtures containing more than 60% of C_2H_2. The C content in these films was in the range 40-100 at.%. The hardness of films increased progressively up to 6 GPa with increasing C_2H_2 concentration in the gas phase or C content in the films (Fig. 5). A reduced hydrogen content in the films was observed to be concomitant with relatively high hardness values. This relatively high hardness may originate from the compressive residual stresses developed in the Cu/a-C:H films. The hardness of a-C:H films produced by microwave plasma-enhanced chemical vapor deposition from pure acetylene was significantly lower than that of composite films (Fig. 5). Tensile residual stresses developed in these films may lead to reduced hardness values.

The hysteresis loop of load-displacement curves for the Cu/a-C:H composite films became less and less pronounced as the C content in the films increased. The elastic recovery of the contact depth during unloading increased considerably. For Cu/a-C:H films produced from pure C_2H_2, approximately 90% of all the indenter displacements originated from the elastic deformation (Fig. 6b). This parameter does not exceed 14% for metal films. The significant increase in harness and very high elastic recovery indicate that the deposition of ion-hardened polymer-like films occurred as the C_2H_2 concentration in the gas phase exceeded 60% [50]. With relatively high C_2H_2 concentrations in the gas phase, the surface of the Cu target was covered with carbon species and these species can be sputtered from the target surface and condensed on the surface of growing films with a relatively high kinetic energy. These energetic species, which condensed on the film surface, may be responsible for the change of properties of films with increasing C_2H_2 concentration in the gas phase. Composite films exhibiting unusual mechanical properties have been deposited under these conditions. The mechanical behavior of these Cu/a-C:H films is close to that of hard rubber. If an abrasive particles moves on the surface of a material with a very high elastic recovery, the elastic deformation of the surface prevails. Therefore, these films having not a very high hardness, but with a very high elastic recovery can possess a high wear resistance [50,52].

3.3 Tribological behavior of copper/carbon films

The friction of coefficient on bare Si surface versus sliding distance was very scattered after the first few cycles under the tribological test conditions investigated (Fig. 7a). This dependence is typical of an abrasive wear. The friction behaviors of pure copper and Cu/a-C:H film containing up to 18 at.% of carbon were rather similar (Fig. 7a). Three distinct

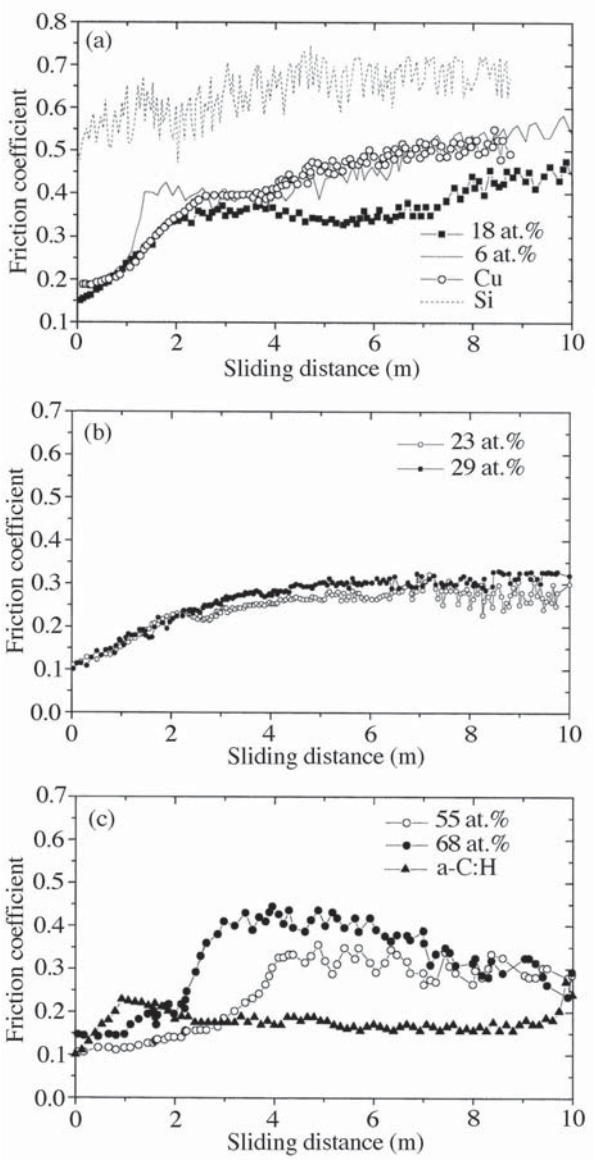

Fig. 7. Friction coefficient versus sliding distance for various samples: (a) bare Si substrate, pure Cu film and Cu/a-C:H films containing 6 and 18 at.% of carbon, (b) Cu/a-C:H films containing 23 and 29 at.% of carbon, and (c) a-C:H film prepared by plasma-assisted chemical vapor deposition from pure C_2H_2 and Cu/a-C:H films containing 55 and 68 at.% of carbon.

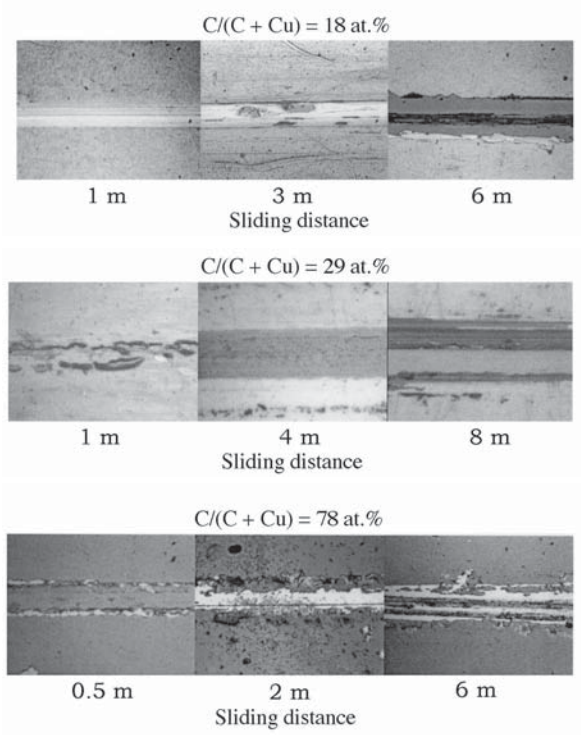

Fig. 8 Optical micrographs of wear tracks for Cu/a-C:H films with a carbon content of : (a) 18 at.%, (b) 29 at.%, and (c) 78 at.% after various sliding distances.

regions can be distinguished depending on the sliding distance. In the initial region corresponding to a sliding distance varying from 0 to 2 m, the initial value of the friction coefficient was in the range 0.15-0.20 and then, the friction coefficient increased linearly with increasing sliding distance. In the meantime, the rider moved on the film surface and penetrated progressively in the films (Fig. 8a, after a sliding distance of 1 m). The increase in friction coefficient with increasing sliding distance was caused by the increase in contact surface area resulting from the gradual penetration of the round surface of the rider into the film.

The value of the friction coefficient was approximately constant as the sliding distance was varied from 2 to 4 m (Fig. 7a). In this region, the rider was sliding on the border of films and smooth Si surface. The optical micrograph of the wear track for a sliding distance of 3 m is given in Fig.8a. The sliding distance value in this region was determined to a greater extent by various phenomena and parameters, such as the transfer of film material to the rider surface, the hardness and viscosity of wear debris, and the adhesion of films to Si substrates. For sliding distances higher than 6 m, the values of the friction coefficient were found relatively scattered (Fig. 7a). In this third region, the rider was sliding directly against the Si surface (Fig. 8a, after a sliding distance of 6 m). Therefore, the length of the sliding distance in the first region corresponds really to a relative measure of the wear resistance of films under the tribological test conditions investigated.

The initial friction coefficient of 0.1 was relatively low for Cu/a-C:H films containing 23 to 29 at.% of carbon and the length of the sliding distance in the first region corresponding the film abrasion increased considerably (Fig. 7b). The friction coefficient for sliding distance of 10 m and above did not exceeded 0.35. A sharp increase in friction coefficient was not observed between the second and third regions of friction tests. The optical micrograph of the wear track displayed a partial foliation of films in the first region of friction (Fig. 8b, after a sliding distance of 1 m). For high sliding distances, the wear track exhibited a smoother surface (Fig. 8b, after sliding distances of 4 and 8 m). This smooth surface of the wear track, reduced friction coefficient and increased wear resistance may result from the change of shear stresses during friction as the C content in the films increased. For a-C:H films, the formation of a thin graphite film with a low shear stress in the sliding contact is recognized to be responsible for reduced friction coefficients [53]. Such mechanism leading to a reduction of friction coefficient values can be invoked also for Cu/a-C:H composite films.

The tribological behavior of Cu/a-C:H films with a C content of 55 at.% and above was relatively different (Fig. 7c). In the first region of the tribological tests, the friction coefficient values were scattered and the length of the sliding distance decreased as a result of a reduced wear resistance of films. The wear tracks exhibited spike edges and cracks typical of the wear of hard and brittle films with a weak adhesion on the surface of Si substrates (Fig. 8c). For a-C:H films produced by microwave plasma-assisted chemical vapor deposition from pure C_2H_2, the friction coefficient increased from 0.1 to 0.25 as the sliding distance increased up to 1 m (Fig.7c). Then, the friction coefficient value was relatively stable as the sliding distance was varied from 1 to 10 m and these films exhibited a reduced wear resistance.

4. CONCLUSION

Nanostructured copper/a-C:H composite films with a C content varying from 5 to 99 at.% have deposited on Si substrates from argon-acetylene mixtures using a hybrid technique combining sputter-deposition and microwave plasma-assisted chemical vapor deposition. These films consisted of Cu crystallites embedded in the carbon matrix. The hardness of copper-rich films with a C content lower than 50 at.% was similar to that of pure Cu films. For carbon-rich films, the hardness increased up to 6 GPa with increasing carbon content. The mechanical behavior of these films was close to that of hard rubber, which is very favorable for wear-resistant films. Relatively low friction coefficients equal to approximately 0.1 were obtained from carbon-rich films in room air with a relative humidity of 50%. These films deposited on Si substrates suffered from a drastic limitation since the adhesion was rather poor for tribological tests. However, these films deposited on other substrates with improved adhesion would be appropriate for tribological applications. Additional investigations are in progress to improve the adhesion of these composite films on various substrates.

ACKNOWLEDGMENTS

The financial supports of this work from the French Ministry of Defense (DGA), French Ministry of Research (ACI COMETCAR project and French-Hungarian Balaton program) and NATO (CLG) through the Scientific Affairs Division are gratefully acknowledged.

REFERENCES

[1] I.L. Singer, in: *New Approaches to Tribology : Theory and Applications*, ed. by L.E. Pope, L.L. Fehrenbacher and W.O. Winer (Mater. Res. Soc. Symp. Proc. 140, Pittsburgh, PA, 1989) p.215.
[2] H. Dimigen and H. Hubsch // *Philips Techn. Rev.* **41** (1983/84) 186.
[3] A. Grill // *Wear* **168** (1993) 143.
[4] K.-H. Habig // *Surf. Coat. Technol.* **76/77** (1995) 540.
[5] A. Erdemir, C. Bindal, J. Pagan and P. Wilbur // *Surf. Coat. Technol.* **76/77** (1995) 559.
[6] R. Memming, H.J. Tolle and P.E. Wierenga // *Thin Solid Films* **143** (1986) 31.
[7] K. Enke // *Mater. Sci. Forum* **52/53** (1989) 559.
[8] J. Franks, K. Enke and A. Richardt // *Met. Mater.* Nov. (1990) 695.
[9] A.A. Voevodin, M.S. Donley, J.S. Zabinski and J.E. Bultman // *Surf. Coat. Technol.* **76/77** (1995) 534.
[10] A.A. Voevodin, A.W. Phelps, M.S. Donley and J.S. Zabinski // *Diamond Relat. Mater.* **5** (1996) 1264.
[11] A.A. Voevodin and M.S. Donley // *Surf. Coat. Technol.* **82** (1996) 199.
[12] A.A. Voevodin, S.D. Walck and J.S. Zabinski // *Wear* **203/204** (1997) 516.

[13] H. Dimigen and H. Hubsch, *US Patent 4,525,417, Jun. 25, 1985*.
[14] H. Dimigen, H. Hubsch and R. Memming // *Appl. Phys. Lett.* **50** 1056 (1987).
[15] T. Zehnder and J. Patscheider // *Surf. Coat. Technol.* **133/134** (2000) 138.
[16] J. Patscheider, T. Zehnder and M. Diserens // *Surf. Coat. Technol.* **146/147** (2001) 201.
[17] M. Stüber, H. Leiste, S. Ulrich, H. Holleck and D. Schild // *Surf. Coat. Technol.* **150** (2002) 218.
[18] A.A. Voevodin, M.A. Capano, A.J. Safiet, M.S. Donley and J.S. Zabinski // *Appl. Phys. Lett.* **69** (1996) 188.
[19] A.A. Voevodin, S.V. Prasad and J.S. Zabinski // *J. Appl. Phys.* **82** (1997) 855.
[20] A.A. Voevodin and J.S. Zabinski // *J. Mater. Sci.* **33** (1998) 319.
[21] A.A. Voevodin and J.S. Zabinski // *Thin Solid Films* **370** (2000) 223.
[22] S. Veprek and S. Reiprich // *Thin Solid Films* **268** (1995) 64.
[23] N. Boonthanom and M. White // *Thin Solid Films* **24** (1974) 295.
[24] S.A.Y. Al-Ismail and C.A. Hogarth // *J. Mater. Sci.* **22** (1987) 415.
[25] S.B. Wang, P.R. Zhu and W.J. Wang // *Surf. Coat. Technol.* **123** (2000) 173.
[26] W. Yuguang, Z. Tonghe, Z. Yawen, Z. Gu, Z. Huixing and Z. Xiaoji // *Surf. Coaat. Technol.* **148** (2001) 221.
[27] I. Gerhards, C. Ronning, U. Vetter, H. Hofsäss, H. Gibhardt, G. Eckold, Q. Li, S.T. Lee, Y.L. Huang and M. Seibt // *Surf. Coat. Technol.* **158/159** (2002) 114.
[28] S.J. Dikshit, P. Lele, S.B. Ogale and S.T. Kshirsagar // *J. Mater. Res.* **11** (1996) 2236.
[29] R.A. Roy, R. Messier and S.V. Krishnaswamy // *Thin Solid Films* **109** (1983) 27.
[30] V.I. Ivanov-Omskii, A.V. Tolmatchev and S.G. Yastrebov // *Phil. Mag. B* **73** (1996) 715.
[31] V.I. Ivanov-Omskii, V.I. Siklitskii and S.G. Yastrebov // *Phys. Solid State* **40** (1998) 524.
[32] T.N. Vasilevskaya, N.S. Andreev, I.A. Drozdova, V.N. Filipovich, S.G. Yastrebov, and T.K. Zvonareva // *Phys. Solid State* **41** (1999) 1918.
[33] T. Cabioc'h, A. Naudon, M. Jaouen, D. Thiaudiere and D. Babonneau // *Phil. Mag. B* **79** (1999) 501.
[34] P.A. Chen // *Thin Solid Films* **182** (1989) 261.
[35] P.A. Chen // *Thin Solid Films* **204** (1991) 413.
[36] N.E. Bazieva, S.G. Yastrebov, V.F. Masterov and A.V. Prichodko // *Mol. Mater.* **4** (1994) 143.
[37] W.-Y. Wu and J.M. Ting // *Thin Solid Films* **420/421** (2002) 166.
[38] Y. Pauleau and F. Thiéry // *Mater. Lett.* **56** (2002) 1053.
[39] Y. Pauleau, F. Thiéry, J. Pelletier, V.V. Uglov, A.K. Kuleshov, S.N. Dub and M.P. Samtsov, In: *Nanostructured Materials and Coatings for Biomedical and Sensor Applications*, ed. by Y.G. Gogotsi and I.V. Uvarova, NATO Science Series, Sub-Series II. Mathematics, Physics and Chemistry, Vol.102 (Kluwers Academic Publishers, Dordrecht, The Netherlands, 2003) p.175.
[40] M. Pichot and J. Pelletier, In: *Microwave Excited Plasma*, ed. by M. Moisan and J. Pelletier, Plasma Technology, 4 (Elsevier, Amsterdam, The Netherlands, 1992) Chap.14, p.419.
[41] Y. Pauleau, F. Thiéry, V.V. Uglov, A.K. Kuleshov, S.N. Dub and M.P. Samtsov // *Rev. Adv. Mater. Sci.* **4** (2003) 139.
[42] Y. Pauleau and F. Thiéry // *Surf. Coat. Technol.*, to be published in 2004.
[43] H.P. Klug and L.E. Alexander, *X-Ray Diffraction Procedures for Polycrystalline and Amorphous Materials* (Wiley, New York, 1974).
[44] A. Barna, G. Radnoczi and B. Pecz, In: *Handbook of Microscopy*, ed. by S. Amelinckx, D. van Dyck, J. van Landuyt and G. van Tendelo, Vol.3 (VCH Verlag, 1997) Chap. II/3, p.751.
[45] Y. Pauleau, In: *Deposition and Processing of Thin Films, Handbook of Thin Film Materials*, ed. by H.S. Nalwa, Vol.1 (Academic Press, San Diego, 2002) Chap.9, p.455.
[46] W.C. Oliver and G.M. Pharr // *J. Mater. Res.* **7** (1992) 1564.
[47] F. Thiéry, Y. Pauleau and L. Ortega // *J. Vac. Sci. Technol. A* **22** (2004) 30.
[48] *JCPDS Data Cards,* 04-0836, International Center of Diffraction Data, Swarthmore, PA, 1999.
[49] E.H. Lee, Y. Lee, W.S. Oliver and L.K. Mansur // *J. Mater. Res.* **8** (1997) 377.
[50] N.V. Novikov, M.A. Voronkin, S.N. Dub, I.N. Lupich, V.G. Malogolovets and B.A. Maslyuk // *Diamond Rel. Mater.* **6** (1997) 574.

[51] N. Inagaki, *Plasma Surface Modification and Plasma Polymerization* (Technomic, London, 1996).

[52] J. Esteve, A. Lousa, E. Martinez, H. Huck, E.B. Halak and M. Reinoso // *Diamond Rel. Mater.* **10** (2001) 1053.

[53] Y. Liu, A. Erdemir and E.I. Metelis // *Surf. Coat. Technol.* **86/87** (1996) 564.